AGU PUBLICATIONS

JGR

Journal of Geophysical Research: Oceans

RESEARCH ARTICLE

10.1002/2014JC010643

Temporal and spatial variability of particle transport in the deep Arctic Canada Basin

Jeomshik Hwang[1], Minkyoung Kim[1], Steven J. Manganini[2], Cameron P. McIntyre[3], Negar Haghipour[3], JongJin Park[4], Richard A. Krishfield[2], Robie W. Macdonald[5], Fiona A. McLaughlin[5], and Timothy I. Eglinton[2,3]

[1]School of Earth and Environmental Sciences/Research Institute of Oceanography, Seoul National University, Seoul, South Korea, [2]Woods Hole Oceanographic Institution, Woods Hole, Massachusetts, USA, [3]ETH Zürich, Zürich, Switzerland, [4]Kyungpook National University, Daegu, South Korea, [5]Fisheries and Oceans Canada, Institute of Ocean Sciences, Sidney, British Columbia, Canada

Abstract To better understand the current carbon cycle and potentially detect its change in the rapidly changing Arctic Ocean, we examined sinking particles collected quasi-continuously over a period of 7 years (2004–2011) by bottom-tethered sediment trap moorings in the central Canada Basin. Total mass flux was very low ($<$100 mg m^{-2} d^{-1}) at all sites and was temporally decoupled from the cycle of primary production in surface waters. Extremely low radiocarbon contents of particulate organic carbon and high aluminum contents in sinking particles reveal high contributions of resuspended sediment to total sinking particle flux in the deep Canada Basin. Station A (75°N, 150°W) in the southwest quadrant of the Canada Basin is most strongly influenced while Station C (77°N, 140°W) in the northeast quadrant is least influenced by lateral particle supply based on radiocarbon content and Al concentration. The results at Station A, where three sediment traps were deployed at different depths, imply that the most likely mode of lateral particle transport was as thick clouds of enhanced particle concentration extending well above the seafloor. At present, only 1%–2% of the low levels of new production in Canada Basin surface waters reaches the interior basin. Lateral POC supply therefore appears to be the major source of organic matter to the interior basin. However, ongoing changes to surface ocean boundary conditions may influence both lateral and vertical supply of particulate material to the deep Canada Basin.

Key Points:
- Particle supply to deep Canada Basin was examined based on C-14 and Al contents
- Canada Basin is starved of fresh POC and is fed by lateral supply of old carbon
- SW of Canada Basin was most influenced by lateral input of resuspended sediment

Supporting Information:
- Supporting Information S1
- Data Set S1

Correspondence to:
J. Hwang,
jeomshik@snu.ac.kr

Citation:
Hwang, J., M. Kim, S. J. Manganini, C. P. McIntyre, N. Haghipour, J.J. Park, R. A. Krishfield, R. W. Macdonald, F. A. McLaughlin, and T. I. Eglinton (2015), Temporal and spatial variability of particle transport in the deep Arctic Canada Basin, *J. Geophys. Res. Oceans*, *120*, 2784–2799, doi:10.1002/2014JC010643.

Received 11 DEC 2014
Accepted 18 MAR 2015
Accepted article online 24 MAR 2015
Published online 11 APR 2015

1. Introduction

The physical environment of the Arctic Ocean and surrounding land masses is changing and is projected to be strongly affected by the current climate change [*IPCC*, 2013, and references therein]. Along with many other facets of this system, carbon cycling will likely respond to ongoing changes in physical forcing factors and it may in turn contribute to further climate change through feedback processes [*IPCC*, 2013, and references therein]. Understanding the processes driving the carbon cycle in the Arctic Ocean is of importance for assessing impacts on the ecosystems it supports.

Ongoing decline in sea ice coverage is one phenomenon that will likely affect carbon cycling in the Arctic Ocean. However, very limited data are currently available to assess if and how these effects will be manifested. Decreasing ice cover can potentially enhance primary production because of newly exposed open water and a prolonged growing season [*Bates*, 2006; *Arrigo et al*., 2008; *Nishino et al*., 2011]. On the other hand, enhanced stratification caused by freshwater buildup may prevent nutrient supply to the euphotic zone and limit phytoplankton growth [*McLaughlin and Carmack*, 2010; *Nishino et al*., 2011; *Lalande et al*., 2014]. The latter would imply that the capacity for uptake of atmospheric CO_2 in the Canada Basin would not necessarily increase in the future [*Cai et al*., 2010a; *Nishino et al*., 2011; *Else et al*., 2013], although the stability of this freshwater cap in the Canada Basin is also the subject of debate [*Krishfield et al*., 2014].

The Canada Basin is characterized by the lowest primary production among the Arctic Seas [*Varela et al*., 2013]. In addition, using ^{234}Th, *Cai et al*. [2010b] showed that the ratio of export production over primary production in the central Arctic Ocean was very small, suggesting a tightly coupled Arctic Ocean food web.

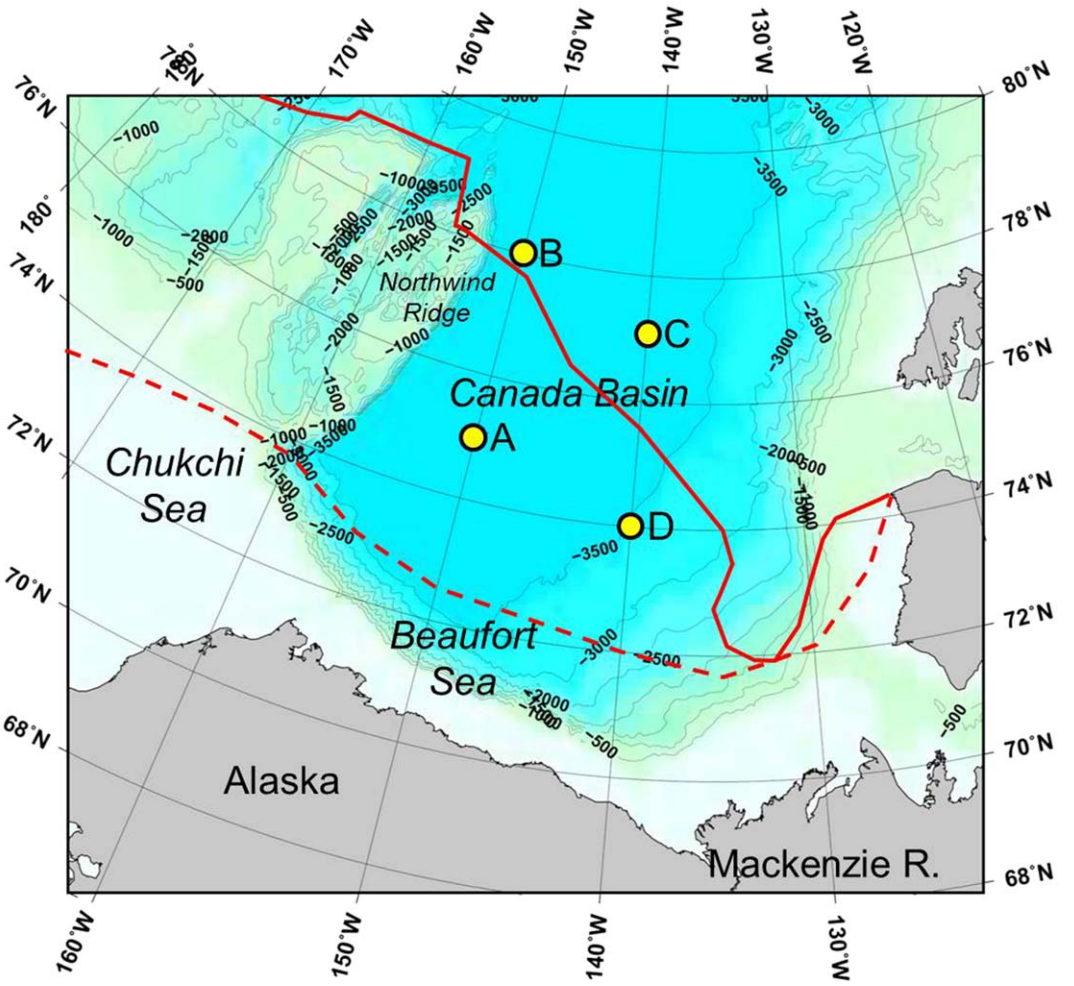

Figure 1. A map of the study area showing the location of the mooring sites. September sea ice extent of 1979–2014 average (dashed line) and in 2008 (solid line) are also shown (http://nsidc.org/data/).

Another study using ice-tethered sediment trap deployments in the deep Arctic basins also showed low POC fluxes at 2–25 m under drifting ice floes [*Lalande et al*., 2014]. *Varela et al*. [2013] showed that new production and the *f* ratio in the Canada Basin were the lowest among the Arctic Seas. Recycling in the euphotic zone or epipelagic zone may change in the future in response to the prolonged exposure to the atmosphere, evolving plankton communities, and coupling/uncoupling between phytoplankton and grazers [*Honjo et al*., 2010; *Hunt et al*., 2014].

We have previously reported flux and POC (particulate organic carbon) isotope (^{13}C and ^{14}C) data for settling particles collected at ~3000 m by a sediment trap deployed on a bottom-tethered mooring at a site in the seasonal sea ice zone in the southwest quadrant of the Canada Basin (Station A in Figure 1) in 2004–2005 [*Hwang et al*., 2008]. We found that the temporal variation in POC flux was decoupled from the seasonal cycle of primary productivity in surface waters, and that sinking particle composition was characterized by ^{14}C-depleted organic carbon (mean ^{14}C age = ~1900 years) and abundant lithogenic material (~80%), implying that the majority of particulate material originated from the surrounding margins. These results suggest that lateral particle supply was a dominant mode of POC delivery to the deep interior of the Canada Basin. However, the extent to which these observations, which stemmed from a 1 year deployment of a single sediment trap at the mooring location, are representative of other sectors of the Canada Basin, and whether they reflect overall temporal variations in particle flux, source, and composition remains uncertain.

Variations in sea ice cover and water circulation pattern caused by changes in air-sea interaction, ice-drag, input of the Pacific warm water, eddies, etcetera may induce spatial and temporal variations in the flux and

composition of particulate matter delivered to the interior Canada Basin. Moreover, it is important to establish particle flux behavior under "baseline" conditions in order to detect abrupt shifts or trajectory changes in response to changing boundary conditions. The mooring site in *Hwang et al*. [2008], located in the seasonal ice zone, is directly affected by the ongoing changes accompanying sea ice retreat. Examining the temporal trend in particle flux, mode of particle supply and particulate matter composition at this site thus provides an opportunity to detect and understand potential carbon cycle perturbations due to the current climate change. We resumed collection of sinking particles in the Canada Basin in 2007, and here we report observations from spatially and temporally more extensive suite of data on the flux and POC ^{14}C contents of settling particles in the Canada Basin.

2. Methods

Sinking particles were collected using time series sediment traps (McLane Research Laboratories, Mark-7) deployed from August 2007 to July 2009 and from September 2010 to September 2011 in different sectors of the Canada Basin (Figure 1). The sediment traps were deployed on bottom-tethered hydrographic moorings operated by the Beaufort Gyre Exploration Project [*Kemp et al*., 2005; *Proshutinsky et al*., 2009]. Station A (75°N, 150°W; total water depth 3825 m; note that this station is different from the hydrographic site "Station A" located at 72.6°N and 144.7°W) is located in the seasonal ice zone of the southwest Canada Basin. Three sediment traps were deployed at 2050, 3100, and 3752 m (50 m above the bottom) from August 2007 to July 2009. From September 2010 to September 2011, only one trap was deployed at 3100 m. At Station B, located further north (78°N, 150°W) in waters covered by ice on a year-round basis during the study, one trap was deployed at 3056 m from August 2007 to July 2009 and from September 2010 to September 2011. At Station C (77°N, 140°W), also currently under permanent ice cover, one trap was deployed at 3047 m from August 2007 to August 2008. Another trap was deployed in the southeast Canada Basin (Station D, 74°N, 140°W) at 2878 m from August 2007 to August 2009. Some of the traps malfunctioned and did not collect samples for all programmed time intervals. Specific sample gaps are: cup #19–21 of 3000 m trap at Station A during the 2010–2011 deployment; cup #19–21 at Station B during both 2007–2008 and 2010–2011 deployments; cup #18–21 at Station C during the 2007–2008 deployment; cup #14–21 at Station D during the 2007–2008 deployment (details of the data can be found in supporting information Data Set S1). Trap deployment depths and sample collection periods are listed in Table 1. Hereafter, nominal depths of 2000, 3000, and 3750 m are used to describe the sampling depths. We previously collected sinking particle samples at 3067 m at Station A from August 2004 to July 2005, and the fluxes, biochemical composition, and carbon isotopic composition of these samples have been reported [*Hwang et al*., 2008; *Honjo et al*., 2010].

Sample cups were filled with seawater fortified with NaCl (about 5 g/L) and poisoned with mercuric chloride (0.3 wt %). Each sample represents about 17 days of collection period (Table 1). Upon recovery, samples were stored at 4°C until subsampling and further analysis. Fractions smaller than 1 mm were used for subsequent investigation. Although we did not determine the contribution of particles >1 mm, most of the samples were devoid of particles in this size fraction and the ones that did had only trace amounts. Sample splitting and preparation for elemental analyses and carbon isotope analysis were described in detail in *Hwang et al*. [2009]. Briefly, samples for flux determination and elemental analyses were filtered onto polycarbonate filters, rinsed with MQ water then air-dried (60°C). We assign a conservative uncertainty of 5% for mass flux measurement (see a review by *Buesseler et al*. [2007] on the use of sediment traps for estimation of sinking particle fluxes). Aluminum (Al) concentration was measured by ICP-ES (Jobin-Yvon Horiba ULTIMA2) [*Honjo et al*., 1995]. Concentration of lithogenic component was estimated by multiplying the Al concentration by 12.15 [*Taylor and McLennan*, 1985; *Honjo et al*., 1995]. Total carbon was analyzed using an elemental analyzer (Perkin-Elmer 2400). Organic carbon content was estimated as the difference between the total carbon and total inorganic carbon, with the latter analyzed by coulometric titration (UIC Coloumetrics equipped with an acidification module CM5130).

Each sample for carbon isotope analysis was freeze-dried after removal of the supernatant. A fraction of each dried sample was dispersed over a precombusted 25 mm GF/F filter in a Petri-dish and exposed to concentrated HCl vapor in a desiccator for $\sim$12 h at room temperature to remove inorganic carbon [*Hedges and Stern*, 1984]. The HCl-treated sample was packed in double quartz tubes with CuO and silver wires,

Table 1. Trap Deployment Location, Sampling Duration, and Cup Opening Interval[a]

Station	Location (Water Depth)	Sampling Duration	Cup Opening Interval (days)	Trap Depth (m)	Total Particle Flux (mg m^{-2} d^{-1})	POC Flux (mg C m^{-2} d^{-1})	Al (%)	$\Delta^{14}C$ (‰)
A	75°N 150°W (3825 m)	13 Aug 2004 to 31 Jul 2005	16.81	3067	11.8 (1.0–37.9, $n = 21$)	0.47 (0.08–1.4, $n = 16$)	6.7 (4.4–7.4, $n = 21$)	−216 (−97 to −257, $n = 11$)
				2050	7.5 (0.27–29.4, $n = 21$)	0.34 (0.19–0.45, $n = 7$)	6.8 (4.4–8.1, $n = 16$)	−155 (−34 to −211, $n = 17$)
		10 Aug 2007 to 1 Aug 2008	17.00	3100	11.9 (0.26–38.0, $n = 21$)	0.89 (0.38–2.3, $n = 15$)	7.0 (6.4–7.8, $n = 16$)	−212 (−31 to −270, $n = 19$)
				3752	13.0 (0.24–28.3, $n = 21$)	0.5 (0.15–1.0, $n = 20$)	7.3 (5.6–8.6, $n = 20$)	−244 (−130 to −277, $n = 19$)
				2050	22.8 (1.0–69.6, $n = 21$)	0.82 (0.02–2.0, $n = 21$)	8.0 (5.7–10.3, $n = 17$)	−276 (−137 to −386, $n = 18$)
		29 Jul 2008 to 21 Jul 2009	17.05	3100	27.0 (3.8–77.4, $n = 21$)	1.1 (0.12–2.6, $n = 16$)	7.5 (5.5–8.4, $n = 16$)	−309 (−209 to −401, $n = 20$)
				3752	31.2 (2.5–92.2, $n = 21$)	1.1 (0.1–3.1, $n = 19$)	7.0 (4.5–8.6, $n = 18$)	−323 (−195 to −410, $n = 19$)
		30 Sep 2010 to 12 Sep 2011	16.50	3100	14.0 (1.3–26.9, $n = 19$)	0.54 (0.1–1.2, $n = 15$)	7.2 (5.2–8.1, $n = 16$)	−276 (−239 to −301, $n = 17$)
B	78°N 150°W (3821 m)	15 Aug 2007 to 7 Aug 2008	17.05	3056	12.2 (1.4–33.6, $n = 18$)	0.54 (0.2–1.1, $n = 15$)	7.3 (6.6–8.0, $n = 12$)	−191 (−72 to −267, $n = 16$)
		2 Aug 2008 to 25 Jul 2009	17.00	3056	7.8 (0.8–17.2, $n = 21$)	0.29 (0.1–0.8, $n = 19$)	7.2 (5.8–8.1, $n = 17$)	−175 (−106 to −231, $n = 19$)
		4 Oct 2010 to 16 Sep 2011	16.50	3056	8.5 (0.6–14.0, $n = 18$)	0.42 (0.1–1.0, $n = 17$)	7.2 (5.9–8.2, $n = 12$)	−189 (−58 to −283, $n = 14$)
C	77°N 140°W (3722 m)	21 Aug 2007 to 10 Aug 2008	16.90	3047	2.3 (0.2–9.2, $n = 17$)	0.26 (0.04–0.70, $n = 5$)	4.5 (1.4–6.0, $n = 4$)	No data
		28 Aug 2007 to 12 Aug 2008	16.67	2878	2.4 (0.3–9.3, $n = 13$)	0.15 (0.03–0.32, $n = 3$)	6.0 (5.1–7.8, $n = 3$)	No data
D	74°N 140°W (3518 m)	15 Aug 2008 to 7 Aug 2009	17.00	2878	4.2 (1.2–10.7, $n = 21$)	0.23 (0.06–0.67, $n = 15$)	7.0 (5.6–7.8, $n = 12$)	−173 (−71 to −206, $n = 9$)

[a]The mean and range of data of each deployment are given for total particle flux, POC flux, Al concentration, and $\Delta^{14}C$ (see supporting information Data Set S1 for a complete data set).

evacuated, flame-sealed, combusted (850°C for 5 h), and the resulting CO_2 gas was cryogenically purified. Both radio-carbon and stable-carbon isotope ratios were measured at the National Ocean Sciences Accelerator Mass Spectrometry (AMS) Facility at Woods Hole Oceanographic Institution [*McNichol et al*., 1994]. Samples analyzed for radiocarbon at ETH, Zürich (indicated in supporting information Data Set S1) were weighed in silver elemental analyzer cups and fumigated with concentrated HCl vapor in a desiccator. The resulting carbonate-free samples were then wrapped in a second tin capsule and graphitized using an AGE system and analyzed on a MICADAS instrument [*Wacker et al*., 2010a, 2010b]. Stable carbon isotopic compositions ($\delta^{13}C$) of the HCl-fumigated samples were measured separately with a stable isotope ratio mass spectrometer (Delta V plus) coupled to a Flash EA 1112 (Thermo) at ETH. The uncertainty based on 11 duplicate radiocarbon analyses obtained at the ETH facility was $\pm 8‰$ (1σ). An interfacility comparison between NOSAMS WHOI and ETH based on 19 and 23 pairs of duplicate analyses resulted in differences (WHOI values minus ETH values) of $9‰ \pm 14‰$ and $0.6‰ \pm 0.4‰$ for $\Delta^{14}C$ and $\delta^{13}C$, respectively.

Other hydrographic results such as current direction and strength are available at the Beaufort Gyre Exploration Project website (http://www.whoi.edu/beaufortgyre/home). Some of the wire-crawling moored profilers (MMP, McLane Research Laboratories, Inc.) were equipped with turbidity sensors. At Station A from August 2007 to July 2008, the MMP repeated vertical migration every 8–10 h. The 1 year time series turbidity data at 2000 m obtained when the MMP was at this depth, were moving-averaged to extract daily values.

3. Results

3.1. Total Mass Flux

3.1.1. Intraannual and Interannual Variations

In describing the intraannual variability, we opted to use each mooring deployment period (i.e., from summer to summer) instead of calendar year. The flux of sinking particles smaller than 1 mm at 3000 m depth at Station A ranged from 0.3 to 77 mg m^{-2} d^{-1} (Figure 2). Seasonal oscillations in particle flux were variable. The data from the 2004–2005 deployment showed a clear distinction between low and high flux

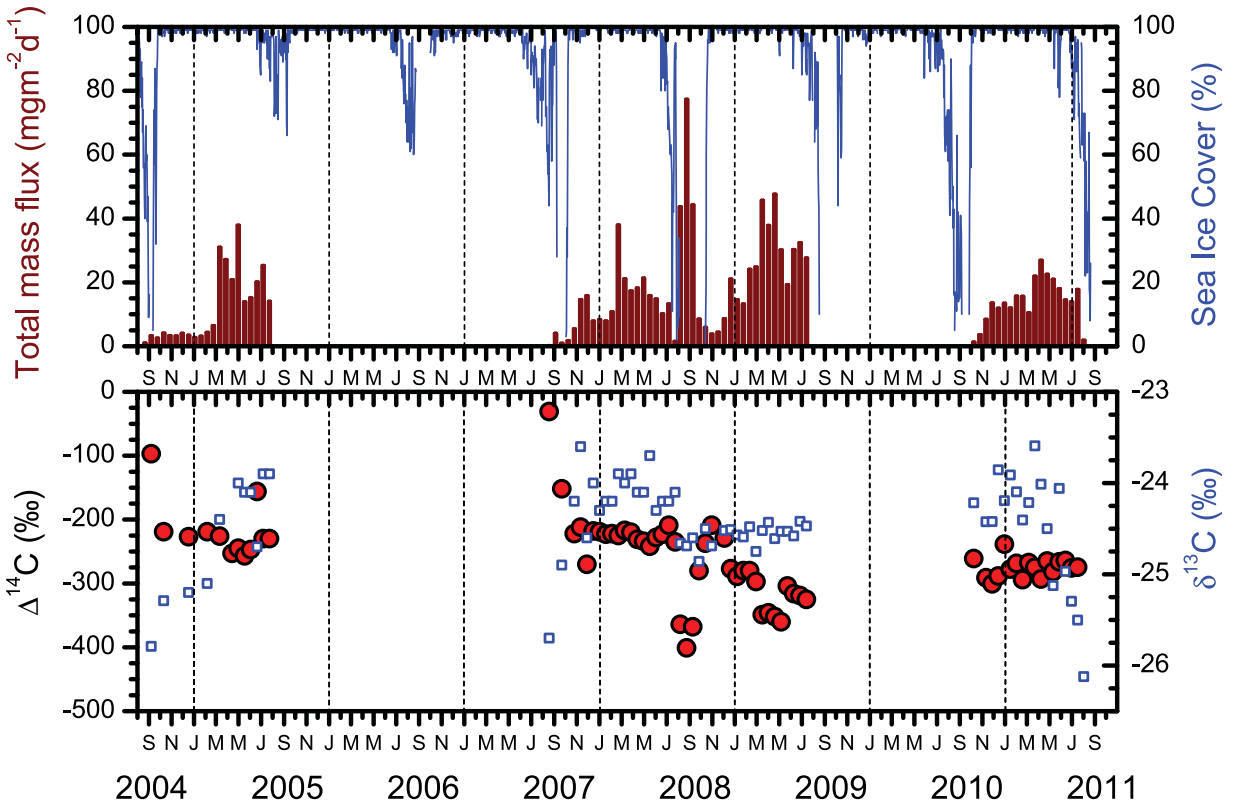

Figure 2. (a) Particle flux at 3100 m depth and sea ice concentration at Station A (data from NOAA) and (b) $\Delta^{14}C$ (circles) and $\delta^{13}C$ (squares) values of sinking POC of the corresponding samples. The data for 2004–2005 are from *Hwang et al.* [2008].

periods for the first (September–February) and second half (March–July) of the study period, respectively. Although this distinction in subsequent deployments was not as clear as in 2004–2005, the flux was generally higher from April to June than from September to February. One exception was an abrupt spike in particle flux (up to 77 mg m^{-2} d^{-1}) observed in August 2008. This conspicuous peak, which was recorded in consecutive sampling cups, contrasts sharply with the low values before and afterward, implying that it reflected a sedimentation event.

The annual average particle flux ($\pm 1\sigma$) at 3000 m in 2007–2008 (11.8 ± 11.2 mg m^{-2} d^{-1}; note that throughout the text the presented variability about the average values reflects temporal variability within the time series, not uncertainty) was similar to that in 2004–2005 (11.9 ± 8.9 mg m^{-2} d^{-1}) and 2010–2011 (14.0 ± 6.9 mg m^{-2} d^{-1}). However, the average flux in 2008–2009 (27.0 ± 18.3 mg m^{-2} d^{-1}) was considerably higher, partly because of the August high flux even. Nevertheless, when the three high values in August and September were excluded, the average flux in 2008–2009 (22.3 ± 13.6 mg m^{-2} d^{-1}), remains higher than those in the other years. For the limited time series thus far, there is no correlation between annual particle flux and sea ice extent.

3.1.2. Vertical Variations

Vertical variations in particle flux were examined from samples collected at three depths by sediment traps deployed for two consecutive years on the Station A mooring (Figure 3). The recorded fluxes were temporally coupled without any apparent phase shift or lag. With only a few exceptions, the flux at 3750 m was similar to, or higher than, those at the other depths. Indeed, the average flux from 2007 to 2009 was 15.2 ± 13.8, 19.2 ± 15.2, and 21.5 ± 18.7 mg m^{-2} d^{-1} at 2000, 3000, and 3750 m, respectively, revealing a general trend of increasing particle flux with depth. The vertical distribution of fluxes can be further grouped into four cases: (i) the fluxes at all depths were similar (e.g., late October 2007 to mid-January 2008; November 2008 to February 2009), (ii) the fluxes at the two shallower depths (2000 and 3000 m) were similar to one another but significantly lower than those at 3750 m (e.g., September–October 2007; and late September–October 2008),

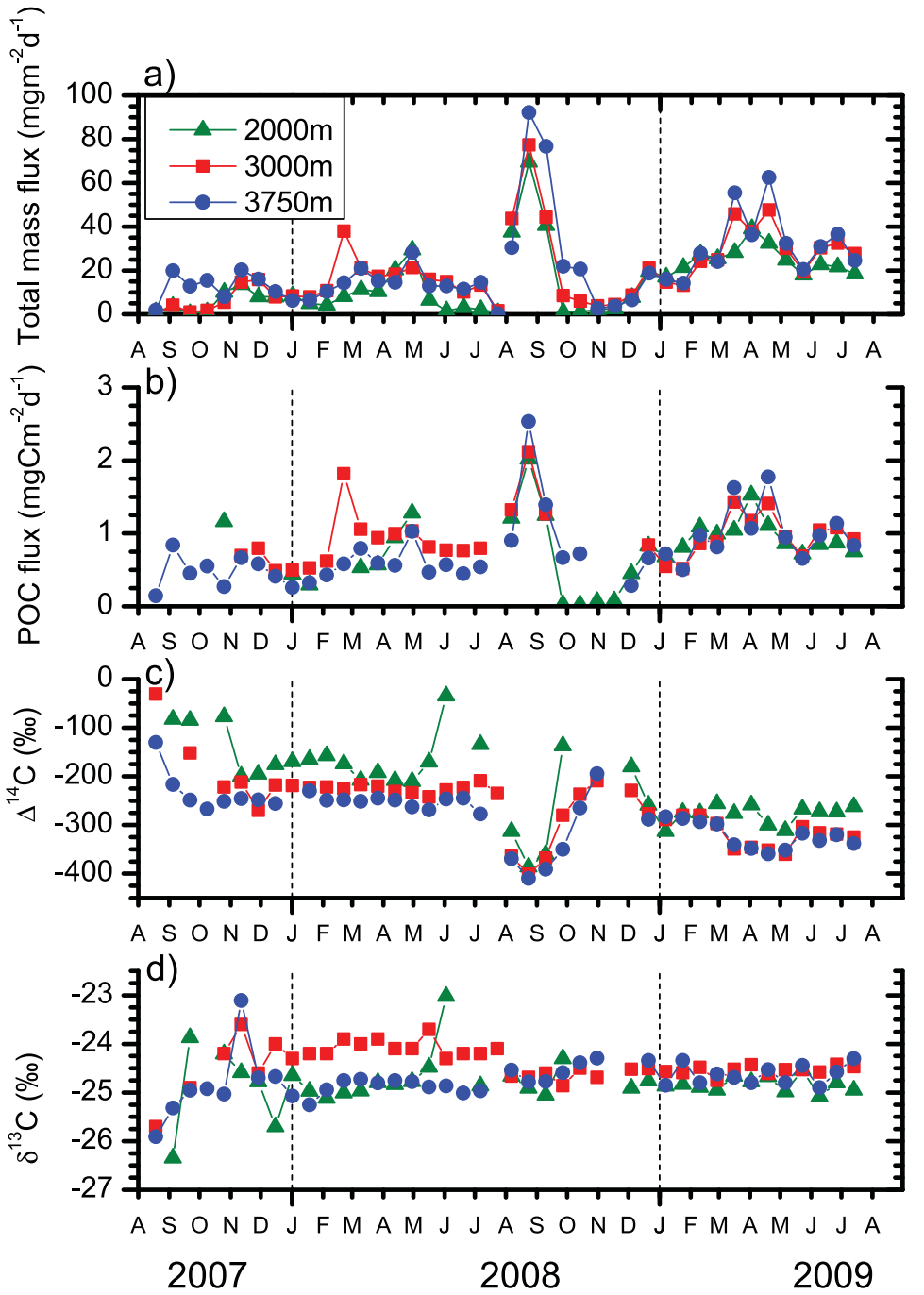

Figure 3. (a) Total mass flux of sinking particles, (b) POC flux, and (c) $\Delta^{14}C$ and (d) $\delta^{13}C$ values of sinking POC at three trap depths at Station A.

(iii) the fluxes at 3000 and 3750 m were similar to one another but considerably higher than those at 2000 m (May–July 2008; and late June–July 2009), and (iv) the fluxes at all depths were different but systematically increased with increasing depth (e.g., late August to early September 2008; March–April 2009). There were two rare cases when the flux at 3000 m was the highest (February and August 2008).

3.1.3. Spatial Variations

Spatial variations in particle flux were assessed from sediment traps located at ~3000 m on moorings deployed in different quadrants of the Canada Basin (Figure 1). At Station B (northwest quadrant), particle flux ranged between 1 and 34 mg m^{-2} d^{-1} with a 3 year average of 9.4 ± 6.3 mg m^{-2} d^{-1} (Figure 4). The

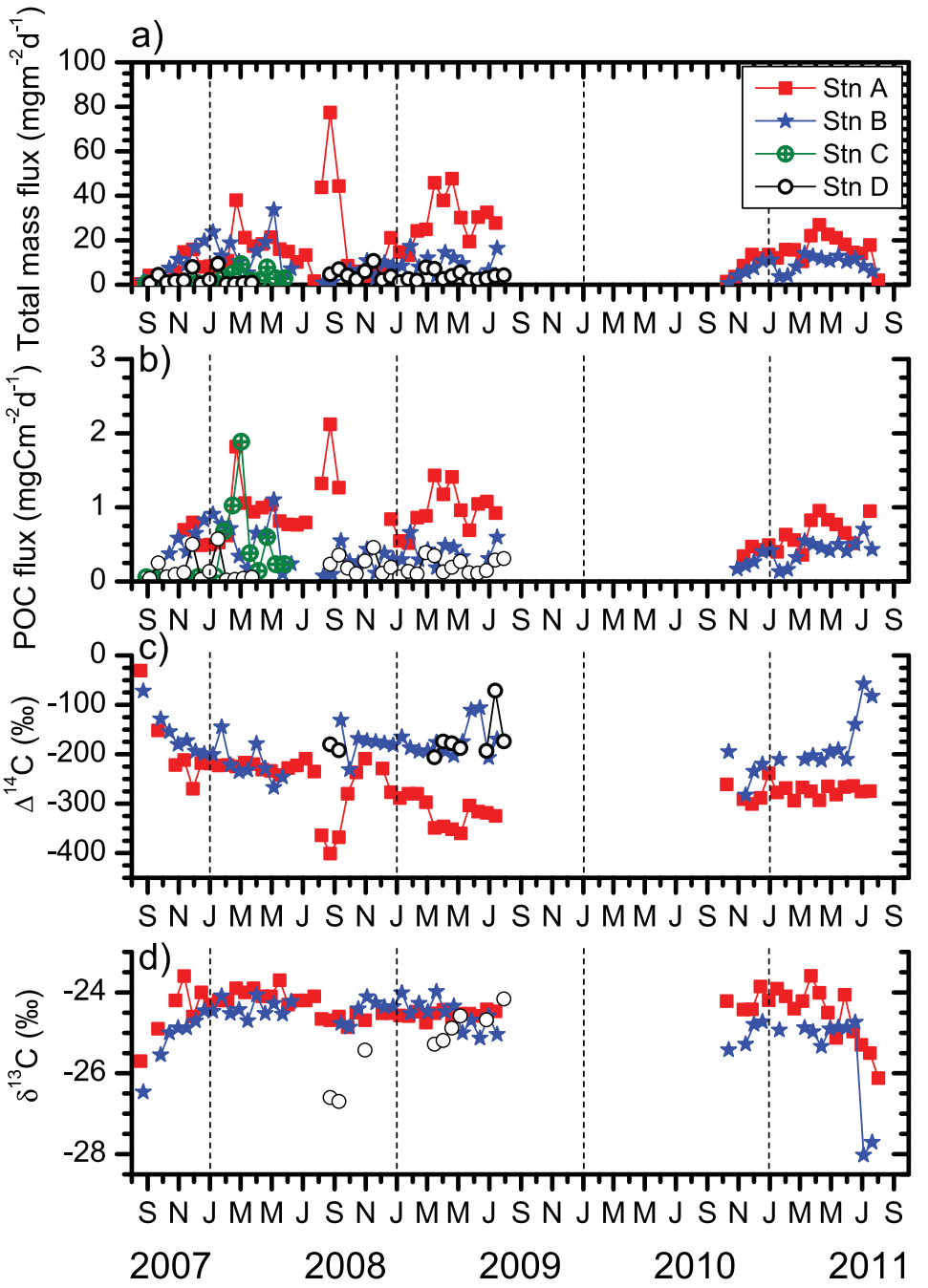

Figure 4. (a) Total mass flux of sinking particles, (b) POC flux, and (c) $\Delta^{14}C$ and (d) $\delta^{13}C$ values of sinking POC at approximately 3000 m in the Canada Basin.

values in 2007–2008 (average = 12.2 mg m^{-2} d^{-1}) were more variable and slightly higher than those in 2008–2009 (average = 7.8 mg m^{-2} d^{-1}) and in 2010–2011 (8.5 mg m^{-2} d^{-1}). The particle flux was extremely low in August and September 2007 (1.4–2.4 mg m^{-2} d^{-1}) and increased in winter and spring (5–34 mg m^{-2} d^{-1}). The highest value was observed in April/May in 2008. The values were comparable to those of Station A in 2007–2008, but lower than those at Station A in 2008–2009 and 2010–2011.

At Station C (northeast quadrant), particle flux in 2007–2008 (2.3 ± 2.7 mg m^{-2} d^{-1} on average) was lower than those at Stations A and B. The particle flux was <1 mg m^{-2} d^{-1} from August until mid-January, after which fluxes were slightly elevated until the end of May (4.3 mg m^{-2} d^{-1} on average for eight samples).

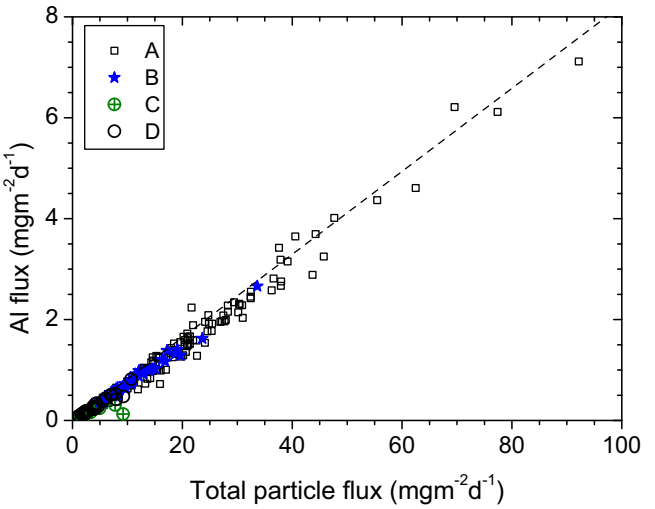

Figure 5. Aluminum flux versus total particle flux. For Station A, data for all three depths were shown as one symbol. The dashed line denotes the case when 100% of sinking material was composed of lithogenic particles, under the assumption of 8.23% Al concentration for clay minerals [*Taylor and McLennan*, 1985].

Particle flux at Station D (southeast quadrant) ranged between 1 and 11 mg m^{-2} d^{-1} (3.5 ± 2.7 mg m^{-2} d^{-1} on average) and did not exhibit any notable seasonal pattern. The particle flux was slightly higher in 2008–2009 (4.2 ± 2.4 mg m^{-2} d^{-1}, $n = 13$) than in 2007–2008 (2.4 ± 3.0 mg m^{-2} d^{-1}).

3.2. Al Concentration

Because there is little influence from eolian dust input in the Canada Basin [*Middag et al.*, 2009; *Macdonald and Gobeil*, 2012], Al can serve as a good proxy for particle supply via sediment resuspension. Al concentrations (Al %) in sinking particles ranged between 4% and 9% (not shown, supporting information Data Set S1), with an exceptionally high value (10.3%) observed in June 2009 at 2000 m at Station A. Seasonally, Al % values in summer were lower than the annual average. The 2007–2009 flux-weighted average Al % value at Station A was 7.9%, 7.4%, and 7.4% at 2000, 3000, and 3750 m, respectively. Al % values at Station C were markedly lower than those at the other sites, implying significant spatial variability in resuspended sediment supply. In general, however, the very high Al % values indicate that lithogenic (aluminosilicate) material comprises the dominant component of the sinking particles (Figure 5). When converted from Al % using the average Al content in the continental crust (8.23%) [*Taylor and McLennan*, 1985], the lithogenic component is estimated to account for over 80% of the sinking particle flux, except for Station C where it accounted for ~46% of the sinking particle flux.

3.3. POC Concentration and Flux

POC content (POC %) in sinking particle samples at Stations A, B, and D mostly ranged between 2.5% and 6.5% (not shown). At Station A, high POC values over 7% were observed during summer periods with the exception of the summer 2008. Although no clear depth trend was observed at Station A, POC % values were generally lowest at 3750 m, with 2 year average POC values of 4.2%, 4.4%, and 3.7%, at 2000, 3000, and 3750 m, respectively. While it should be noted that POC % data are not available for all samples, the limited amount of available measurements indicate that POC % values were considerably higher at Station C than at other sites. POC % of ~20% was observed in January–March at this station. POC % at Station D (average = 5.5) was generally also slightly higher than at Stations A and B.

Seasonal variations in POC flux at 3000 m at Station A were similar to those of the total mass flux (Figure 3), with generally lower POC fluxes in summer (except summer 2008). The 4 year average POC flux at this station and depth was 0.73 ± 0.41 mg C m^{-2} d^{-1}.

POC fluxes at three depths at Station A were similar and were temporally coupled, as noted for total mass flux (Figure 3). The average POC flux for 2 years from 2007 to 2009 was 0.80 ± 0.47, 0.96 ± 0.38, and 0.76 ± 0.46 mg C m^{-2} d^{-1} at 2000, 3000, and 3750 m, respectively. There was not any clear trend in POC flux with depth.

POC flux was spatially heterogeneous in the Canada Basin (Figure 4). The annual average POC flux was highest at Station A (4 year average = 0.73 ± 0.41 mg C m^{-2} d^{-1}) followed by Station B (3 year average = 0.42 ± 0.22 mg C m^{-2} d^{-1}). At Station C, the 1 year average POC flux was 0.33 ± 0.49 mg C m^{-2} d^{-1}. At Station D, the 2 year average POC flux, 0.20 ± 0.14 mg C m^{-2} d^{-1}, was lowest among the stations.

3.4. Carbon Isotope Ratios

The $\Delta^{14}C$ values of POC (<1 mm) at 3000 m at Station A ranged from −31‰ to −401‰ (Figure 2). The highest value was observed in August/September 2007 when the ice concentration was rapidly decreasing.

With the exception of the high values in summer 2004 and summer 2007, $\Delta^{14}C$ values were uniformly low (about $-230‰$), exhibiting only minor variation ($\sigma = 14‰$) until August 2008 when $\Delta^{14}C$ values decreased to $-364‰$ and remained low for three consecutive samples. The $\Delta^{14}C$ values at Station A in 2007–2008 exhibited a similar seasonal pattern as in 2004–2005: the values were considerably higher during sea ice melt in late summer than in the other seasons when values were uniformly low. Also POC collected during the period characterized by low $\Delta^{14}C$ values (November–June) in the two study periods yielded remarkably similar average $\Delta^{14}C$ values: $-229‰ \pm 29‰$ in 2004–2005 versus $-227‰ \pm 14‰$ in 2007–2008. However, 2008–2009 period was different from the previous years. First, in place of higher values, the lowest value was observed in August when the anomalous peak in particle flux was observed (Figure 2). Second, the average $\Delta^{14}C$ value was significantly lower than those in the previous years and seasonal variability was also much higher compared to the previous study periods. In 2010–2011, $\Delta^{14}C$ values were within a narrow range and the average value ($-276‰ \pm 15‰$) was lower than that of 2004–2005 or 2007–2008.

$\Delta^{14}C$ values for POC collected at different depths at Station A showed a vertical trend. With only one exception (January 2009), the $\Delta^{14}C$ value at 2000 m was higher than the corresponding values at 3000 and 3750 m for each sampling interval (Figure 3c). The average $\Delta^{14}C$ values were $-217‰ \pm 82‰$, $-262‰ \pm 70‰$, $-284‰ \pm 58‰$ at 2000, 3000, 3750 m, respectively, exhibiting a decreasing trend with increasing sampling depth. The $\Delta^{14}C$ values at 3750 m were on average lower than those at 2000 m by $\sim 60‰$ (± 31, $n = 27$).

At Station B, the $\Delta^{14}C$ values ranged between $-58‰$ and $-283‰$ (Figure 4). The $\Delta^{14}C$ values in August 2007 and July 2011 were considerably higher than the annual average values. The average $\Delta^{14}C$ value for 3 years was $-183‰ \pm 46‰$. The $\Delta^{14}C$ values at Station B were higher than those at Station A in 2008–2009 and 2010–2011. At Station D, the limited available ^{14}C data were comparable to those at Station B, including a higher value ($-71‰$) in July 2009. The annual average of the available data for Station D was $-173‰ \pm 40‰$.

Stable carbon isotopic compositions ($\delta^{13}C$ values) of POC collected at 3000 m at Station A ranged between $-23.6‰$ and $-26.2‰$ (Figure 2). Lower $\delta^{13}C$ values were observed in summer, and coincided with those periods characterized by high $\Delta^{14}C$ values. In contrast to the prior and subsequent years, significant temporal variability in $\delta^{13}C$ values, and in particular, lower $\delta^{13}C$ values, were not observed in the summer 2008. The temporal variability in $\delta^{13}C$ values during the 2008–2009 period was lower ($\sigma = \pm 0.1‰$) and the values were on average slightly lower than those in the other periods. Vertically, the average $\delta^{13}C$ values at Station A were $-24.8‰ \pm 0.5‰$, $-24.4‰ \pm 0.5‰$, and $-24.8‰ \pm 0.4‰$ at 2000, 3000, and 3750 m, respectively (Figure 3). Seasonal variation in $\delta^{13}C$ values at all stations was not observed, with the exception of the occurrence of lowest values in summer (Figure 4). The average $\delta^{13}C$ value at Stations B and D was -24.8 ± 0.8 and -25.3 ± 0.7, respectively.

4. Discussion

4.1. Particle Flux to the Deep Canada Basin

Measured particle fluxes in the Canada Basin were uniformly low. The average total mass flux at 3000 m, which was 16.2, 9.4, 2.3, and 3.5 mg m^{-2} d^{-1} at Stations A, B, C, and D, respectively, compares with a global average biogenic particle flux of 68 mg m^{-2} d^{-1} for the mesopelagic/bathypelagic boundary of 2000 m (converted from data in *Honjo et al.* [2008]). This low value at 3000 m compared to the global average value at 2000 m is not due to flux attenuation because at Station A, where sediment traps were deployed at different depths, the mass flux at 2000 m was generally similar to or lower than that at 3000 m. Corresponding POC fluxes at 3000 m (0.73, 0.42, 0.33, and 0.20 mg C m^{-2} d^{-1} at Stations A, B, C, and D, respectively) are also much smaller than the global average of 4 mg C m^{-2} d^{-1} for the mesopelagic/bathypelagic boundary [*Honjo et al.*, 2008].

The stations in the western basin appear to be influenced by additional particle supply in winter and spring more than the stations in the eastern basin. Spatial variability in particle flux may reflect seasonal variations in ice cover and associated primary productivity, lateral supply of resuspended sediments, and the distance from land and the shelf break. Primary production in summer is highest in the southwestern part of the Canada Basin [*Nishino et al.*, 2011; *Varela et al.*, 2013; *Hunt et al.*, 2014], and hence the spatial distribution of the observed particle flux is consistent with that of primary production. However, the summer POC flux

comprised only a minor portion of the annual POC flux. Instead, the abundance of lithogenic material (over 80% at Stations A, B, and D, and 46% at Station C) and extremely low $\Delta^{14}C$ values imply that the major fraction of the sinking particulate flux derives from lateral supply of resuspended sedimentary particles emanating from the adjacent margin. Interestingly, no evidence of POC flux derived from ice algal biomass was found unlike elsewhere in the Arctic Ocean [*Boetius et al*., 2013]. Also, no evidence for sea ice transport of coarse material was found.

The generally higher, but more variable, particle fluxes and POC $\Delta^{14}C$ values at Station A appear to be a reflection of its relative proximity to the continental shelf and to the region where eddies are formed [e.g., *Watanabe et al*., 2014], compared to the other stations. Average sedimentation rates at sites near Station A in the Canada Abyssal Plain (at 74°43.5′N, 156°08.5′W and adjacent stations) during the late Holocene were estimated to be less than 1 cm/kyr [*Grantz et al*., 1996]. This is equivalent to a flux of about 20 mg m^{-2} d^{-1} when estimated from the relationship between the sedimentation rate and total sediment accumulation rate during the Holocene at various sites in the Arctic Ocean [*Stein et al*., 2004]. The observed average particle flux at 50 m above the bottom (3750 m) at Station A, 22 mg m^{-2} d^{-1}, is identical to this average sediment accumulation rate, and implies that the current mode of particle flux has persisted, at least since the late Holocene.

Station B is the northernmost site, and permanently ice covered, but located within 100 km of the northern end of the Northwind Ridge (Figure 1). Particle fluxes at this site were lower than that at Station A but also exhibited considerable temporal variability in a manner that is decoupled from the seasonal cycle of photosynthetically active radiation. Peaks of particle flux at Stations A and B (about 330 km apart) do not appear to be correlated, potentially suggesting different provenance of laterally advected particles. Both stations exhibited comparable concentrations of the lithogenic component (about 7.3% of flux-weighted Al concentration), yet considerably different $\Delta^{14}C$ values (flux-weighted average, $-278‰$ and $-184‰$ at Stations A and B, respectively) (Figure 4).

Station C is the most distal mooring from the Beaufort Shelf and also expected to be least influenced by ongoing sea ice retreat given that this site remains covered with sea ice even during the September sea ice minimum. Contributions of lithogenic material were lowest, and therefore it is not surprising that the particle flux was the lowest at this location, although average POC % values were twice that measured at the other stations. Station D, located at the base of the Mackenzie Fan and closest to the mouth of the Mackenzie River, did not show any sign of a spring discharge (freshet) event even though this system is the largest fluvial source of sediment to the Arctic Ocean, supplying 124×10^9 kg of sediment per year into the Beaufort shelf [*Holmes et al*., 2002].

On a $\delta^{13}C$-$\Delta^{14}C$ plot, surface sediments in the adjacent North American Arctic margin are positioned on a linear mixing line between aged terrestrial organic matter and modern marine organic matter [*Goni et al*., 2013, Figure 6]. Our sinking POC samples are located between this mixing line and surface water suspended POC in the Canada Basin on the same plot (Figure 6), implying that the sinking POC is a mixture between these two types of organic matter. The provenance of the laterally transported particles in the Canada Basin is currently under investigation using an expanded suite of geochemical tracers.

4.2. Mode of Lateral Particle Transport in the Southwest Canada Basin

$\Delta^{14}C$ values of suspended POC collected at Stations A and B in summer 2008 by in situ filtration showed a large vertical gradient [*Griffith et al*., 2012]. Reported $\Delta^{14}C$ values of suspended POC near the surface were within $30‰$ of the value of dissolved inorganic carbon and exhibited a gradual decrease with increasing depth with values deeper than 500 m varying between $-50‰$ and $-300‰$ [*Griffith et al*., 2012]. This implies greater influence of aged POC at depth. An interesting observation is that the $\Delta^{14}C$ values of suspended POC were higher than those of sinking POC from similar depths, which is the opposite of what is usually observed in the oceanic environments [*Druffel et al*., 1992; *Hwang et al*., 2004]. The suspended POC samples were collected at Station A on 27 July 2008, 2 days before the collection of sinking POC started at the same location. Hence it is possible that the collection of suspended POC preceded the plume of particles responsible for the enhanced particle flux in August and September of that year. It should be noted however that these suspended POC results only represent a snapshot and clearly further work is warranted.

Hints into the mode of particle transport to Station A can be gleaned from flux data from the sediment traps deployed at three depths on this mooring over a period of 2 years. Particularly notable is the coherence

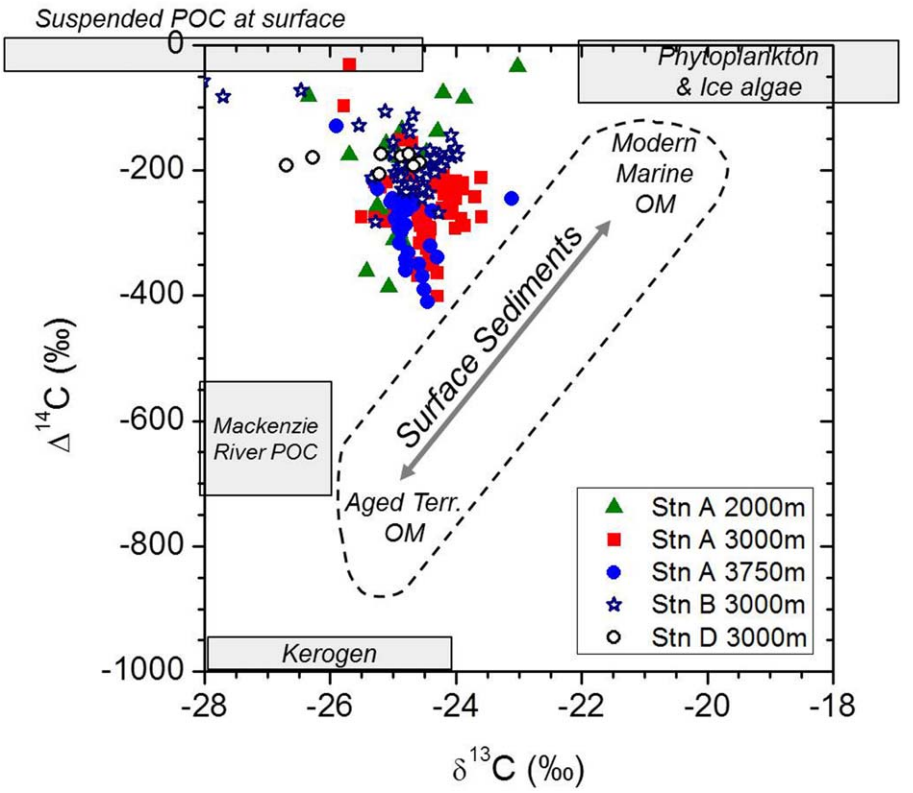

Figure 6. A plot of $\Delta^{14}C$ versus $\delta^{13}C$ of sinking POC. Data for surface sediments and other types of organic matter are borrowed from *Goni et al.* [2013, and references therein]. Results of suspended POC collected in the surface mixed layer of the Canada Basin in 2008 and 2009 [*Brown et al.*, 2014] are also shown.

between particle flux variations at different depths, with no indication of any phase shift between 2000 and 3750 m (Figure 3). This observation implies either that particles responsible for the flux were sinking rapidly (more than several tens of meters per day) or that they are supplied laterally. Such high sinking speeds of particles would appear incompatible with long-distance transport (>350 km) of resuspended sediment from the surrounding shelf to Station A. The latter possibility would imply simultaneous lateral transport of particles as a "cloud" extending at least 1800 m upward from the seafloor.

Northward moving eddies that typically extend downward a few hundred meters through the water column [e.g., *Spall et al.*, 2008; *Timmermans et al.*, 2008; *Watanabe*, 2011], entrain particles on the western Arctic shelves and the upper slope, and shed their particle load during their migration [*O'Brien et al.*, 2011, 2013; *Watanabe et al.*, 2014]. If this were the case, particle fluxes would be expected to decrease or at most remain constant with increasing depth, which contrasts with our observation that particle fluxes generally increase with increasing depth. However, *Zhang et al.* [2014] reported near-bottom sediment transport by mesoscale eddies in the South China Sea: interestingly, these authors report elevated suspended particle concentration near the bottom (2069 m, 30 m above the bottom) without any coincident increase at 617 m depth. Eddies may play a role in mobilization of surface sediment from the shelf and upper slope and in injection of resuspended particles into the basin interior. Resulting particle suspensions could subsequently be transported further to the interior basin via deep currents [*Newton and Coachman*, 1974]. Basin-ward movement of particles thus appears to take place via tall clouds of elevated particle concentration with the thickness of this layer apparently varying considering the observed difference in particle flux at different depths. For example, periods when fluxes to the 3000 and 3750 m traps were similar to one another but considerably higher than that at 2000 m suggest the upper boundary of the cloud was located between 2000 and 3000 m. Such features appear to persist for 1–2 months. During the 2007–2008 deployment, a wire-crawling moored profiler (MMP) equipped with a turbidity sensor show increased signal intensity in September 2007, January, March, and April in 2008 (turbidity data at 2000 m are presented in Figure 7). High particle flux values in March and April generally coincided with signal of enhanced turbidity although

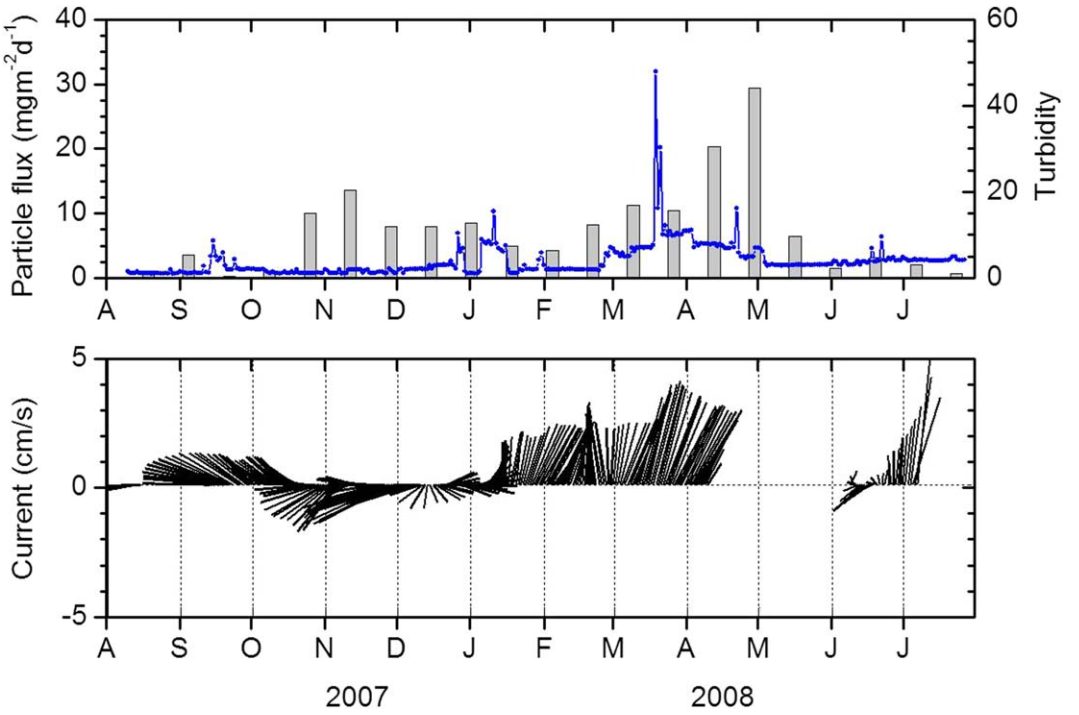

Figure 7. (a) Total particle flux (gray histograms) and turbidity (blue line) and (b) current direction and speed at 2000 m at Station A from August 2007 to July 2008.

there were periods when the correlation was not apparent. This may be because the backscatter sensor was biased toward larger particles and may not see much of the very fine-grained particles.

The aforementioned interpretation generally agrees with the observed relationship between the high particle flux and current direction at Station A suggested from the study during the 2004–2005 period—the period of increased particle flux abruptly started in March with a northward shift in the current direction [*Hwang et al*., 2008]. The current data at 2000 m obtained from Station A in 2007–2008 (Figure 7) showed similar temporal variation of the current direction to that of the 2004–2005 period. The current direction for roughly the first half of the 2007–2008 sampling period (from August to January) was westward and/or southward and then turned toward the north and maintained a predominantly northward trajectory for about 3 months during which higher particle fluxes were observed. However, the shift in current direction and increase in mass flux did not occur synchronously implying more complex relationship between the current direction and mass flux. The current measured by an MMP at Station A does not appear to reflect passage of an eddy in winters when high particle flux was observed. Unfortunately, no current data are available for the 2008–2009 period to relate the conspicuously high flux in August and September in 2008. The cause of this dramatic difference in particle flux in summer 2008 is not clear but may be a consequence of altered deep circulation. The surface water circulation was different between the summers in 2007 and 2008. Dynamic height in the vicinity of Station A was higher in summer 2008 than in summer 2007 implying stronger clockwise circulation in the Canada Basin [*McLaughlin et al*., 2011, Figure 3]. Interdecadal variation of the Arctic Ocean Oscillation [*McLaughlin et al*., 2011] may play a role in lateral transport of particles, although this aspect warrants further investigation.

4.3. Contribution of Allochthonous Particles to Sinking Particle Flux

A substantial proportion of the annual average POC flux to 3000 m at Station A must originate from aged organic matter given the low $\Delta^{14}C$ values (flux-weighted average $\Delta^{14}C = -278‰$, ^{14}C age = ~2550 years). *Hwang et al*. [2008] used $-260‰$ as the end-member for the aged POC, which was an estimated value considering the relationship between aluminum concentration and $\Delta^{14}C$ of sinking particles. However, even lower values than this assumed end-member value have subsequently been observed in 2008–2009 and 2010–2011 (Figure 2). These low values may suggest either (i) that the previous estimate of the $\Delta^{14}C$

Table 2. Properties of the Allochthonous and Autochthonous End-Members Used for Mass Balance Calculation and Contribution of Each Source to Total Sinking Particle Flux and POC Flux at Stations A and D

	Allochthonous End-Member	Autochthonous End-Member	Station A	Station D
$\Delta^{14}C$ (‰)	−420	+30[a]	−278	−173
POC (%)	2.5	20	3.9	5.3
Al % (lithogenic component %)	7.716 (93.75)	0 (0)	7.3 (88.7)	6.7 (81.2)
% Contribution of allochthonous source to total particles and POC (in parentheses)			95 (69)	87 (45)

[a]From *Griffith et al.* [2012].

end-member was too high and consequently, the estimate of the contribution of aged POC was too high or (ii) that the aged POC that affected 2008–2009 samples had a different $\Delta^{14}C$ value, potentially because of a different sediment provenance [cf. *Goni et al.*, 2013]. Determination of end-member values and utilization of isotopic mass balance for source apportionment is therefore subject to considerable uncertainty in the absence of additional constraints on particle provenance.

We adopted the lowest observed $\Delta^{14}C$ value in August 2008 (−420‰, POC % = ~2.5%, resulting Al % = 7.72%) as the potential end-member of the allochthonous POC. This $\Delta^{14}C$ value is not unreasonable considering the range of $\Delta^{14}C$ values of surface sediments in the surrounding margin (Figure 6) [*Goni et al.*, 2013]. The Al % value of this end-member happens to be identical to the average Al concentration in the sediment (7.73% ± 1.48%) collected mainly in and around the Canada Basin [*Macdonald and Gobeil*, 2012]. It is important to bear in mind that there are significant spatial variations in the concentration and ^{14}C content of OC as well as in clay content and Al concentration in sediments [*Macdonald and Gobeil*, 2012; *Goni et al.*, 2013; *Jerosch*, 2013]. The $\Delta^{14}C$ value observed for dissolved inorganic carbon at Station A (+30‰) was adopted as the fresh POC end-member [*Griffith et al.*, 2012]. In this case, a POC % value of ~20% for the vertically transported fresh POC end-member can satisfy the observed POC %, Al %, and $\Delta^{14}C$ values at both Stations A and D. Based on two end-member mixing model using the above end-member values (Table 2), about 69% and 45% of sinking POC, corresponding to 0.23 and 0.10 mg C m^{-2} d^{-1} at Stations A and D, respectively, are estimated to have originated from lateral advection. When the total mass is considered, a much higher proportion (about 95% and 87% at Stations A and D, respectively, in our model, Table 2) of the particles is estimated to be supplied via lateral transport.

It should be borne in mind that the allochthonous source signal may be modified during resuspension and lateral transport. Changing properties of the resuspended sediment particles could take place, for example, by organic matter desorption/sorption processes on clay minerals [e.g., *Satterberg et al.*, 2003]. Such processes may be responsible for the relatively high POC % of the allochthonous end-member and explain the scatter observed in a $\Delta^{14}C$ versus Al concentration plot that defines the mixing line between the two end-members (Figure 8). In this context, particles supplied to Stations A and B could have the same origin while their corresponding $\Delta^{14}C$ and POC % values differ as a consequence of alteration processes during the transit. Again, additional constraints on the provenance of both mineral and organic constituents of laterally advected particles are necessary to resolve this question.

It has been suggested that the POC flux in the upper water column of the central Arctic Ocean is efficiently retained rather than exported to the deep interior [*Wassmann et al.*, 2004]. Recent data are also consistent with this notion [*Cai et al.*, 2010b; *Varela et al.*, 2013]. Average depth-integrated primary production and new production in the outer Beaufort Sea and in the Canada Basin was estimated to be 48 and 14 mg C m^{-2} d^{-1}, respectively, with a corresponding *f* ratio of 0.27 [*Varela et al.*, 2013]. Our estimated flux of fresh sinking POC (excluding laterally advected POC) to 3000 m at Stations A and D corresponds to 1%–2% of this already-low level of new production.

Overall, the deep Canada Basin appears distinct from other ocean basins: the interior basin is starved in vertical POC supply and is fed mainly by lateral transport of POC [see *Timothy et al.*, 2013 for relevant discussion at Station Papa]. There appears to be much dampened flux of POC that carries an old (^{14}C-depleted) signal (−220‰ ± 50‰). Additional supply of fresh POC (more positive $\Delta^{14}C$ values) by vertical settling and aged POC (more negative $\Delta^{14}C$ values) by lateral transport appears to modify this background flux of POC. In terms of POC supply to the deep interior of the basin, at present, lateral supply appears to be at least as

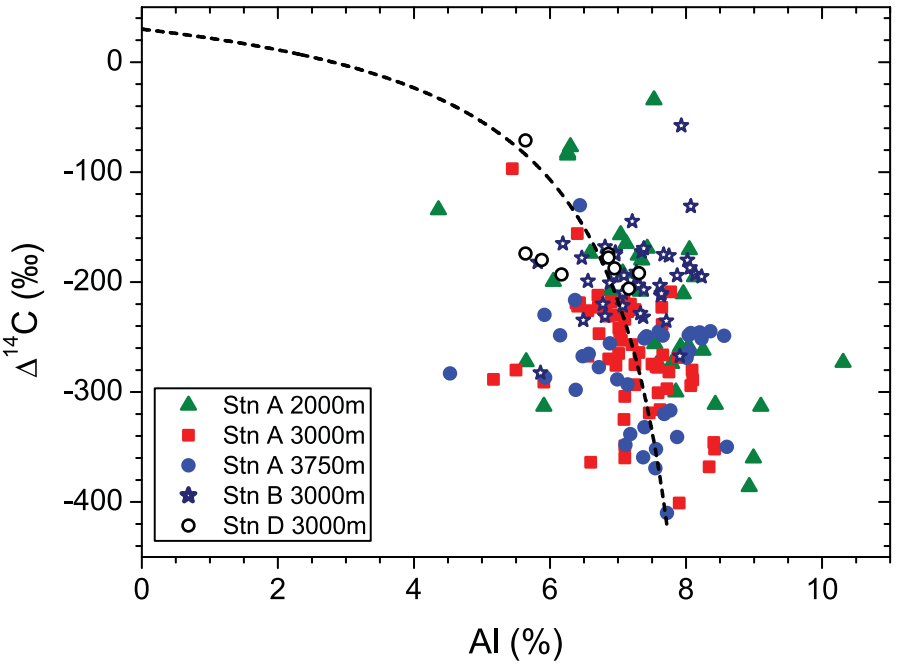

Figure 8. $\Delta^{14}C$ values versus Al concentration. The dashed line denotes a mixing line between the two end-members (see text for detail).

important as fresh POC that is produced in the overlying water column and delivered by biological pump processes in the deep Canada Basin.

5. Summary and Conclusions

We examined the flux and carbon isotopic composition of sinking particles collected at four different locations in the central Canada Basin that are characterized by contrasting surface sea ice conditions and distance from land and shelf break. The measurements extend and augment previously reported data from 2004 to 2005 for a single depth and location in the southwestern quadrant of the basin, and include periods in 2007 and 2008 with record minima in sea ice extent in the Pacific sector of the Arctic Ocean. The results generally confirm the observations and interpretations of *Hwang et al.* [2008] that (i) overall, mass and POC fluxes are very low relative to other ocean basins and (ii) lateral particle supply is a predominant feature of particle flux processes in this basin, supplying lithogenic material and aged POC.

The short duration of the observations and significant interannual variability in particle fluxes preclude identification of secular trends in POC flux, and signals will also be muted by flux attenuation at the sediment trap deployment depths (3000 m). Nevertheless, no apparent change in freshly produced POC from the overlying water column in summer was detected during our limited observation period, despite the aforementioned intervals of minimum sea ice extent. Moreover, in contrast to recent observations elsewhere in the central Arctic Ocean, there were no indications of episodic pulses of increased biogenic matter flux such as derived from ice algal blooms. An interesting phenomenon was the occurrence of a pulse of particulate material in summer 2008 that was characterized by even lower $\Delta^{14}C$ values, implying that it was caused by enhanced sediment resuspension and transport.

Extremely low $\Delta^{14}C$ values of sinking POC were observed at all three sites indicating that supply of aged POC from the continental margin as the major source of POC was widespread in the deep Canada Basin. These $\Delta^{14}C$ values, which are among the lowest observed in any ocean basin, underline the importance of lateral supply of aged POC to this basin. Carbon isotopic measurements in sediment traps deployed at different locations in the basin reveal that lateral supply of particles was spatially heterogeneous, with the greatest magnitude and variability in lateral particle flux evident in the southwestern Canada Basin. These observations suggest that this quadrant of the basin is affected by episodic input of laterally transported particles from the adjacent margin. Settling particles in the southeast quadrant showed no evidence of

direct influence from the Mackenzie River. The vertical distribution of mass flux and $\Delta^{14}C$ values for sinking particles collected at three depths in the southwest basin suggests that particles were laterally transported from the margin as a thick cloud extending over 1800 m above the seafloor, however the underlying processes remain unclear.

Overall, the deeper regions of the basin (e.g., >2000 m) appears to be a reservoir of suspended matter that is replenished by vertical flux from above plus horizontal flux from the sides and disaggregation within the water column. The sinking particle flux is modulated by addition of faster sinking particles either supplied vertically or horizontally. Contributions of laterally supplied particulate material to total sinking particle flux was estimated to be over 85%, and contributions to sinking POC was 69% and 45% in the southwest and southeast quadrants, respectively, based on radiocarbon mass balance. Comparing POC fluxes corrected for this lateral supply with reported values for surface ocean productivity, we estimate that approximately 1%–2% of new production reaches the deep interior of the Canada Basin. This compares with a global average of about 8% to the mesopelagic/bathypelagic boundary of 2000 m [*Honjo et al*., 2008], and implies the operation of an inefficient biological pump at present in the central Arctic Ocean.

Lateral supply of resuspended particles is likely influenced by multiple factors. The role of the surface and deep ocean processes on the lateral transport of particles from the continental margin to the basin interior, and potential impacts of future changes to these processes, warrants further investigation.

Acknowledgments

We thank D. Montluçon (ETH) for guidance in laboratory work, D. Montluçon and D.R. Griffith (WHOI) for fieldwork, S. Bishop (ETH) for assistance with $\delta^{13}C$ measurements, the Laboratory for Ion Beam Physics (ETH) for access to Accelerator Mass Spectrometry facilities, the WHOI Mooring Operations and Engineering Group, A. Proshutinsky for support as the PI of Beaufort Gyre Exploration Project, W. Williams and S. Zimmermann for their contributions as chief scientists of the JOIS cruises, the captain and crew of the CCGS *Louis S. St. Laurent*, and Fisheries and Oceans Canada for logistical support. Sea ice extent data were retrieved from http://nsidc.org/data/. This research was funded by the NSF Division of Polar Programs (ARC-0909377), the Ocean and Climate Change Institute of Woods Hole Oceanographic Institution, and ETH Zürich. J.H. and M.K. were partly supported by the National Research Foundation of Korea grant funded by the Korean Government (2011–0013629).

References

Arrigo, K. R., G. van Dijken, and S. Pabi (2008), Impact of a shrinking Arctic ice cover on marine primary production, *Geophys. Res. Lett.*, *35*, L19603, doi:10.1029/2008GL035028.

Bates, N. R. (2006), Air-sea CO_2 fluxes and the continental shelf pump of carbon in the Chukchi Sea adjacent to the Arctic Ocean, *J. Geophys. Res.*, *111*, C10013, doi:10.1029/2005JC003083.

Boetius, A., et al. (2013), Export of algal biomass from the melting Arctic sea ice, *Science*, *339*, 1430–1432.

Brown, K. A., F. A. McLaughlin, P. D. Tortell, D. E. Varela, M. Yamamoto-Kawai, B. Hunt, and R. Francois (2014), Determination of particulate organic carbon sources to the surface mixed layer of the Canada Basin, Arctic Ocean, *J. Geophys. Res. Oceans*, *119*, 1084–1102, doi:10.1002/2013JC009197.

Buesseler, K. O., et al. (2007), An assessment of the use of sediment traps for estimating upper ocean particle fluxes, *J. Mar. Res.*, *65*, 345–416.

Cai, P., M. Rutgers van der Loeff, I. Stimac, E.-M. Nothig, K. Lepore, and S. B. Moran (2010b), Low export flux of particulate organic carbon in the central Arctic Ocean as revealed by ^{234}Th:^{238}U disequilibrium, *J. Geophys. Res.*, *115*, C10037, doi:10.1029/2009JC005595.

Cai, W.-J., et al. (2010a), Decrease in the CO_2 uptake capacity in an ice-free Arctic Ocean basin, *Science*, *329*, 556–559.

Druffel, E. R. M., P. M. Williams, J. E. Bauer, and J. R. Ertel (1992), Cycling of dissolved and particulate organic matter in the open ocean, *J. Geophys. Res.*, *97*, 15,639–15,659.

Else, B. G. T., R. J. Galley, B. Lansard, D. G. Barber, K. A. Brown, L. A. Miller, A. Mucci, T. N. Papakyriakou, J.-E. Tremblay, and S. Rysgaard (2013), Further observations of a decreasing atmospheric CO_2 uptake capacity in the Canada Basin (Arctic Ocean) due to sea ice loss, *Geophys. Res. Lett.*, *40*, 1132–1137, doi:10.1002/grl.50268.

Goni, M. A., A. E. O'Connor, Z. Z. Kuzyk, M. B. Yunker, C. Gobeil, and R. W. Macdonald (2013), Distribution and sources of organic matter in surface marine sediments across the North American Arctic margin, *J. Geophys. Res. Oceans*, *118*, 4017–4035, doi:10.1002/jgrc.20286.

Grantz, A., R. L. Phillips, M. W. Mullen, S. W. Starratt, G. A. Jones, A. S. Naidu, and B. P. Finney (1996), Character, paleoenvironment, rate of accumulation, and evidence for seismic triggering of Holocene turbidities, Canada Abyssal Plain, Arctic Ocean, *Mar. Geol.*, *133*, 51–73.

Griffith, D. R., A. P. McNichol, L. Xu, F. A. McLaughlin, R. W. Macdonald, K. A. Brown, and T. I. Eglinton (2012), Carbon dynamics in the western Arctic Ocean: Insights from full-depth carbon isotope profiles of DIC, DOC, and POC, *Biogeosciences*, *9*, 1217–1224.

Hedges, J. I., and J. H. Stern (1984), Carbon and nitrogen determinations of carbonate-containing solids, *Limnol. Oceanogr.*, *29*, 657–663.

Holmes, R. M., J. McClelland, B. J. Peterson, I. A. Shiklomanov, A. I. Shiklomanov, A. V. Zhulidov, V. V. Gordeev, and N. N. Bobrovitskaya (2002), A circumpolar perspective on fluvial sediment flux to the Arctic Ocean, *Global Biogeochem. Cycles*, *16*(4), 1098, doi:10.1029/2001GB001849.

Honjo, S., J. Dymond, R. Collier, and S. J. Manganini (1995), Export production of particles to the interior of the equatorial Pacific Ocean during the 1992 EqPac experiment, *Deep Sea Res., Part II*, *42*, 831–870.

Honjo, S., S. J. Manganini, R. A. Krishfield, and R. Francois (2008), Particulate organic carbon fluxes to the ocean interior and factors controlling the biological pump: A synthesis of global sediment trap programs since 1983, *Prog. Oceangr.*, *76*, 21–285.

Honjo, S., R. A. Krishfield, T. I. Eglinton, S. J. Manganini, J. N. Kemp, K. Dpherty, J. Hwang, T. K. McKee, and T. Takizawa (2010), Biological pump processes in the cryopelagic and hemipelagic Arctic Ocean: Canada Basin and Chukchi Rise, *Prog. Oceangr.*, *85*, 137–170.

Hunt, B. P. V., R. J. Nelson, B. Williams, F. A. McLaughlin, K. V. Young, K. A. Brown, S. Vagle, and E. C. Carmack (2014), Zooplankton community structure and dynamics in the Arctic Canada Basin during a period of intense environmental change (2004–2009), *J. Geophys. Res. Oceans*, *119*, 2518–2538, doi:10.1002/2013JC009156.

Hwang, J., E. R. M. Druffel, S. Griffin, K. L. Smith, R. J. Baldwin, and J. E. Bauer (2004), Temporal variability of $\Delta^{14}C$, $\delta^{13}C$, and C/N in sinking particulate organic matter at a deep time series station in the northeast Pacific Ocean, *Global Biogeochem. Cycles*, *18*, GB4015, doi:10.1029/2004GB002221.

Hwang, J., T. I. Eglinton, R. A. Krishfield, S. J. Manganini, and S. Honjo (2008), Lateral organic carbon supply to the deep Canada Basin, *Geophys. Res. Lett.*, *35*, L11607, doi:10.1029/2008GL034271.

Hwang, J., S. J. Manganini, D. B. Montlucon, and T. I. Eglinton (2009), Dynamics of particle export on the Northwest Atlantic margin, *Deep Sea Res., Part I*, *56*, 1792–1803.

IPCC (2013), Climate change 2013, in *The Physical Science Basis*, edited by T. F. Stocker, et al., Cambridge Univ. Press, Cambridge, U. K.

Jerosch, K. (2013), Geostatistical mapping and spatial variability of surficial sediment types on the Beaufort Shelf based on grain size data, *J. Mar. Syst.*, *127*, 5–13.
Kemp, J., K. Newhall, W. Ostrom, R. Krishfield, and A. Proshutinsky (2005), The Beaufort gyre observing system 2004: Mooring recovery and deployment in pack ice, *Tech. Rep. WHOI-2005-05*, Woods Hole Oceanogr. Inst., Woods Hole, Mass.
Krishfield, R., A. Proshutinsky, K. Tateyama, W. J. Williams, E. C. Carmack, F. A. McLaughlin, and M.-L. Timmermans (2014), Deterioration of perennial sea ice in the Beaufort Gyre from 2003 to 2012 and its impact on the oceanic freshwater cycle, *J. Geophys. Res. Oceans*, *119*, 1271–1305, doi:10.1002/2013JC008999.
Lalande, C., E.-M. Nöthig, R. Somavilla, E. Bauerfeind, V. Shevchenko, and Y. Okolodkov (2014), Variability in under-ice export fluxes of biogenic matter in the Arctic Ocean, *Global Biochem. Cycles*, *28*, 571–583, doi:10.1002/2013GB004735.
Macdonald, R. W., and C. Gobeil (2012), Manganese sources and sinks in the Arctic Ocean with reference to periodic enrichments in basin sediments, *Aquat. Geochem.*, *18*, 565–591.
McLaughlin, F., E. Carmack, A. Proshutinsky, R. D. Krishfield, C. Guay, M. Yamamoto-Kawai, J. M. Jackson, and B. Williams (2011), The rapid response of the Canada Basin to climate forcing, *Oceanography*, *24*, 146–159.
McLaughlin, F. A., and E. C. Carmack (2010), Deepening of the nutricline and chlorophyll maximum in the Canada Basin interior, 2003–2009, *Geophys. Res. Lett.*, *37*, L24602, doi:10.1029/2010GL045459.
McNichol, A. P., E. A. Osborne, A. R. Gagnon, B. Fry, and G. A. Jones (1994), TIC, TOC, DIC, DOC, PIC, POC-unique aspects in the preparation of oceanographic samples for ^{14}C-AMS, *Nucl. Instrum. Methods Phys. Res., Sect. B*, *92*, 162–165.
Middag, R., H. J. W. de Baar, P. Laan, and K. Bakker (2009), Dissolved aluminium and the silicon cycle in the Arctic Ocean, *Mar. Chem.*, *115*, 176–195.
Newton, J. L., and L. K. Coachman (1974), Atlantic Water circulation in the Canada Basin, *Arctic*, *27*, 297–303.
Nishino, S., T. Kikuchi, M. Yamamoto-Kawai, Y. Kawaguchi, T. Hirawake, and M. Itoh (2011), Enhancement/reduction of biological pump depends on ocean circulation in the sea-ice reduction regions of the Arctic Ocean, *J. Oceanogr.*, *67*, 305–314.
O'Brien, M. C., H. Melling, T. F. Pedersen, and R. W. Macdonald (2011), The role of eddies and energetic ocean phenomena in the transport of sediment from shelf to basin in the Arctic, *J. Geophys. Res.*, *116*, C08001, doi:10.1029/2010JC006890.
O'Brien, M. C., H. Melling, T. F. Pedersen, and R. W. Macdonald (2013), The role of eddies on particle flux in the Canada Basin of the Arctic Ocean, *Deep Sea Res., Part I*, *71*, 1–20.
Proshutinsky, A., R. Krishfield, and D. Barber (2009), Preface to special section on Beaufort Gyre Climate System Exploration Studies: Documenting key parameters to understand environmental variability, *J. Geophys. Res.*, *114*, C00A08, doi:10.1029/2008JC005162.
Satterberg, J., T. S. Arnarson, E. J. Lessard, and R. G. Keil (2003), Sorption of organic matter from four phytoplankton species to montmorillonite, chlorite and kaolinite in seawater, *Mar. Chem.*, *81*, 11–18.
Spall, M. A., R. S. Pickart, P. S. Fratantoni, and A. J. Plueddemann (2008), Western Arctic shelfbreak eddies: Formation and transport, *J. Phys. Oceanogr.*, *38*, 1644–1668.
Stein, R., C. Schubert, R. W. Macdonald, K. Fahl, H. R. Harvey, and D. Weiel (2004), The central Arctic Ocean: Distribution, sources, variability and burial of organic carbon, in *The Organic Carbon Cycle in the Arctic Ocean*, edited by R. Stein and R. W. Macdonald, pp. 295–314, Springer, Berlin.
Taylor, S. R., and S. M. McLennan (1985), *The Continental Crusts: Its Composition and Evolution*, Blackwell Sci., Oxford, U. K.
Timmermans, M.-L., J. Toole, A. Proshutinsky, R. Krishfield, and A. J. Plueddemann (2008), Eddies in the Canada Basin, Arctic Ocean, observed from ice-tethered profilers, *J. Phys. Oceanogr.*, *38*, 133–145.
Timothy, D. A., C. S. Wong, J. E. Barwell-Clarke, J. S. Page, L. A. White, and R. W. Macdonald (2013), Climatology of sediment flux and composition in the subarctic Northeast Pacific Ocean with biogeochemical implications, *Prog. Oceanogr.*, *116*, 95–129.
Varela, D. E., D. W. Crawford, I. A. Wrohan, S. N. Wyatt, and E. C. Carmack (2013), Pelagic primary productivity and upper ocean nutrient dynamics across Subarctic and Arctic Seas, *J. Geophys. Res. Oceans*, *118*, 7132–7152, doi:10.1002/2013JC009211.
Wacker, L., M. Christl, and H.-A. Synal (2010a), Bats: A new tool for AMS data reduction, *Nucl. Instrum. Methods Phys. Res., Sect. B*, *268*, 976–979.
Wacker, L., G. Bonani, M. Friedrich, I. Hajdas, B. Kromer, M. Nemec, M. Ruff, M. Suter, H.-A. Synal, and C. Vockenhuber (2010b), MICADAS: Routine and high-precision radiocarbon dating, *Radiocarbon*, *52*, 252–262.
Wassmann, P., et al. (2004), Particulate organic carbon flux to the Arctic Ocean sea floor, in *The Organic Carbon Cycle in the Arctic Ocean*, edited by R. Stein and R. W. Macdonald, pp. 101–138, Springer, Berlin.
Watanabe, E. (2011), Beaufort shelf break eddies and shelf-basin exchange of Pacific summer water in the western Arctic Ocean detected by satellite and modeling analyses, *J. Geophys. Res.*, *116*, C08034, doi:10.1029/2010JC006259.
Watanabe, E., et al. (2014), Enhanced role of eddies in the Arctic marine biological pump, *Nat. Commun.*, *5*, 3950.
Zhang, Y., Z. Liu, Y. Zhao, W. Wang, J. Li, and J. Xu, (2014), Mesoscale eddies transport deep-sea sediments, *Sci. Rep.*, *4*, 5937.